Inorg. Chem. **2004**, *43*, 3921–3929

Dinuclear Ruthenium and Iron Complexes Containing Palladium and Platinum with Tri-*tert*-Butylphosphine Ligands: Synthesis, Structures, and Bonding

Richard D. Adams,*,† Burjor Captain,† Wei Fu,† Michael B. Hall,‡ Mark D. Smith,† and Charles Edwin Webster‡

Department of Chemistry and Biochemistry and the USC NanoCenter, University of South Carolina, Columbia, South Carolina 29208, and Department of Chemistry, Texas A&M University, College Station, Texas 77843-3255

Received March 13, 2004

The reaction of $Pd(PBu^t_3)_2$ with $Ru(CO)_5$ yielded the dipalladium–diruthenium cluster complex $Ru_2(CO)_9[Pd(PBu^t_3)]_2$, **10**. The reaction of $Pt(PBu^t_3)_2$ with $Ru(CO)_5$ at room temperature afforded the diplatinum–diruthenium cluster complex $Ru_2(CO)_9[Pt(PBu^t_3)]_2$, **12**, and the monoplatinum–diruthenium cluster $PtRu_2(CO)_9(PBu^t_3)$, **11**. All three complexes contain a diruthenium group with bridging $Pd(PBu^t_3)$ or $Pt(PBu^t_3)$ groups. Compound **11** can be converted to **12** by reaction with an additional quantity of $Pt(PBu^t_3)_2$. The reaction of **12** with hydrogen at 68 °C yielded the dihydrido complex $Pt_2Ru_2(CO)_8(PBu^t_3)_2(\mu\text{-}H)_2$, **13**. This complex contains a Ru_2Pt_2 cluster with hydride ligands bridging two of the Ru–Pt bonds. The reaction of $Fe_2(CO)_9$ with $Pt(PBu^t_3)_2$ yielded the platinum–diiron cluster complex $PtFe_2(CO)_9(PBu^t_3)$, **14**, which is analogous to **11**. All new complexes were characterized crystallographically. Molecular orbital calculations of **10** reveal an unusual delocalized metal–metal bonding system involving the $Pd(PBu^t_3)$ groups and the $Ru_2(CO)_9$ group.

Introduction

Bimetallic cluster complexes have been shown to be good precursors for the preparation of bimetallic nanoparticles on supports,[1−8] and in some cases these supported bimetallic nanoparticles have been shown to be superior catalysts for hydrogenation reactions.[9,10]

In the past two decades there have been major advances in the syntheses of di- and polynuclear−metal cluster complexes.[11] Recently, we have shown that reactions of $M(PBu^t_3)_2$, M = Pd and Pt, with ruthenium and ruthenium−platinum carbonyl complexes by addition of $M(PBu^t_3)$

* Author to whom correspondence should be addressed. E-mail: Adams@mail.chem.sc.edu.
† University of South Carolina.
‡ Texas A&M University.

(1) Toshima, N.; Yonezawa, T. *New J. Chem.* **1998**, 1179.
(2) Johnson, B. F. G. *Coord. Chem. Rev.* **1999**, *192*, 1269.
(3) Midgley, P. A.; Weyland, M.; Thomas, J. M.; Johnson, B. F. G. *Chem. Commun.* **2001**, 907.
(4) Nashner, M. S.; Frenkel, A. I.; Somerville, D.; Hills, C. W.; Shapley, J. R.; Nuzzo, R. G. *J. Am. Chem. Soc.* **1998**, *120*, 8093.
(5) Nashner, M. S.; Frenkel, A. I.; Adler, D. L.; Shapley, J. R.; Nuzzo, R. G. *J. Am. Chem. Soc.* **1997**, *119*, 7760.
(6) Shephard, D. S.; Maschmeyer, T.; Johnson, B. F. G.; Thomas, J. M.; Sankar, G.; Ozkaya, D.; Zhou, W.; Oldroyd, R. D.; Bell, R. G. *Angew. Chem., Int. Ed. Engl.* **1997**, *36*, 2242.
(7) Raja, R.; Sankar, G.; Hermans, S.; Shephard, D. S.; Bromley, S.; Thomas, J. M.; Johnson, B. F. G. *Chem. Commun.* **1999**, 1571.
(8) Shephard, D. S.; Maschmeyer, T.; Sankar, G.; Thomas, J. M.; Ozkaya, D.; Johnson, B. F. G.; Raja, R.; Oldroyd, R. D.; Bell, R. G. *Chem.—Eur. J.* **1998**, *4*, 1214.
(9) (a) Thomas, J. M.; Johnson, B. F. G.; Raja, R.; Sankar, G.; Midgley, P. A. *Acc. Chem. Res.* **2003**, *36*, 20. (b) Braunstein, P.; Rose, J. In *Catalysis by Di- and Polynuclear Metal Cluster Complexes*; Adams, R. D., Cotton, F. A., Eds.; VCH: New York, 1998; Chapter 13, p 443.
(10) (a) Raja, R.; Khimyak, T.; Thomas, J. M.; Hermans, S.; Johnson, B. F. G. *Angew. Chem., Int. Ed.* **2001**, *40*, 4638. (b) Hermans, S.; Raja, R.; Thomas, J. M.; Johnson, B. F. G.; Sankar, G.; Gleeson, D. *Angew. Chem., Int. Ed.* **2001**, *40*, 1211. (c) Raja, R.; Sankar, G.; Hermans, S.; Shephard, D. S.; Bromley, S.; Thomas, J. M.; Johnson, B. F. G.; Maschemeyer, T. *Chem. Commun.* **1999**, 1571.
(11) (a) Adams, R. D. In *Comprehensive Organometallic Chemistry II*; Abel, E. W., Stone, F. G. A., Wilkinson, G., Eds.; Pergamon: Oxford, 1995; Vol. 10, p 1. (b) Adams, R. D. In *The Chemistry of Metal Cluster Complexes*; Shriver, H. D., Kaesz, H. D., Adams, R. D., Eds.; VCH: New York, 1990; Chapter 3, p 121. (c) Roberts, D. A.; Geoffroy, G. L. In *Comprehensive Organometallic Chemistry II*; Wilkinson, G., Stone, F. G. A., Abel, E. W., Eds.; Pergamon: Oxford, 1995; Vol. 6, Chapter 40, p 763. (d) Farrugia, L. J. *Adv. Organomet. Chem.* **1990**, *31*, 301. (e) Pignolet, L. H.; Aubart, M. A.; Craighead, K. L.; Gould, R. A. T.; Krogstad, D. A.; Wiley: J. S. *Coord. Chem. Rev.* **1995**, *143*, 219. (f) Xiao, J. L.; Puddephatt, R. J. *Coord. Chem. Rev.* **1995**, *143*, 457. (g) Lee, S.-M.; Wong, W.-T. *J. Cluster Sci.* **1998**, *9*, 417.

10.1021/ic049675j CCC: $27.50
Published on Web 06/02/2004

groups, M = Pd and Pt, across the metal−metal bonds provide a convenient and facile new route for the synthesis of these bimetallic cluster complexes.[12] For example, $Pd(PBu^t_3)_2$ and $Pt(PBu^t_3)_2$ react with $Ru_5(CO)_{15}(\mu_5\text{-C})$ to yield the adducts $Ru_5(CO)_{15}(C)[M(PBu^t_3)]$, **1**, M = Pd, and **2**, M = Pt. Both compounds exist in solution as a mixture of open and closed isomers (e.g., **2a** and **2b**) that undergo rapid exchange on the NMR time scale at room temperature.[12b,c] The dipalladium complex $Ru_5(CO)_{15}(\mu_6\text{-C})[Pd(PBu^t_3)]_2$, **3**, was prepared by the addition of two $Pd(PBu^t_3)$ groups to $Ru_5(CO)_{15}(\mu_5\text{-C})$ and engages in similar dynamical processes.[12c] Compound **2** reacts with PhC_2H to yield the complex $PtRu_5(CO)_{13}(\mu_3\text{-}PhC_2H)(PBu^t_3)(\mu_5\text{-C})$, which is a catalyst for the homogeneous hydrogenation of PhC_2H to styrene.[12e]

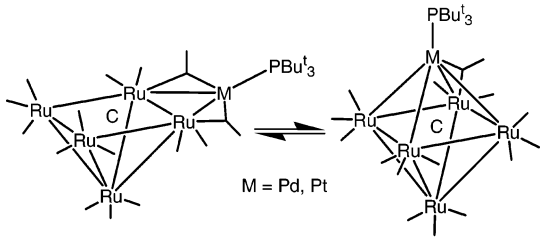

2a **2b**

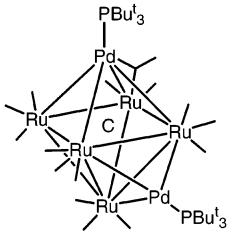

3

We have also shown that $Pd(PBu^t_3)$ and $Pt(PBu^t_3)$ groups will add across Ru−Pt bonds in the mixed-metal cluster $PtRu_5(CO)_{16}(\mu_6\text{-C})$ to afford the adducts $PtRu_5(CO)_{16}(\mu_6\text{-C})[M(PBu^t_3)]_n$, **4** and **5**, where M = Pd and $n = 1$ or $n = 2$, respectively, and **6** and **7**, where M = Pt and $n = 1$ or $n = 2$, respectively.[12d]

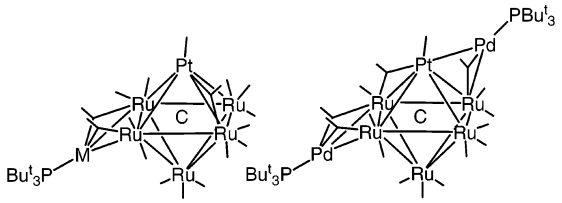

4 M = Pd
6 M = Pt

5

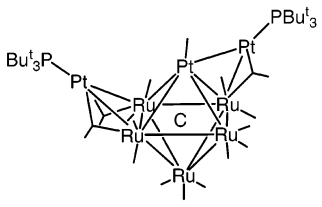

7

In an earlier paper, we reported on the reactions of $Ru_3(CO)_{12}$, $Ru_6(CO)_{17}(\mu_6\text{-C})$, and $Ru(CO)_5$ with $Pd(PBu^t_3)_2$, which yielded the complexes $Ru_3(CO)_{12}[Pd(PBu^t_3)]_3$, **8**, $Ru_6(CO)_{17}(\mu_6\text{−C})[Pd(PBu^t_3)]_2$, **9**, and $Ru_2(CO)_9[Pd(PBu^t_3)]_2$, **10**, respectively, at room temperature.[12a]

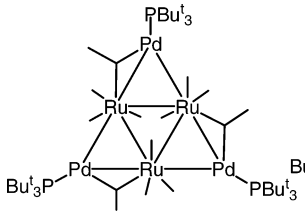

8

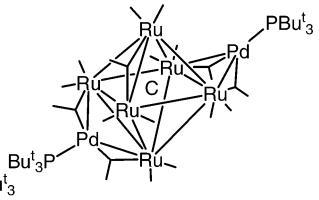

9

We have now investigated the reaction of $Ru(CO)_5$ with $Pt(PBu^t_3)_2$, which yields the diruthenium−platinum complexes $PtRu_2(CO)_9(PBu^t_3)$, **11**, and $Ru_2(CO)_9[Pt(PBu^t_3)]_2$, **12**. The reaction of compound **12** with hydrogen yielded the tetranuclear dihydrido cluster complex $Pt_2Ru_2(CO)_8(PBu^t_3)_2(\mu\text{-H})_2$, **13**. We have also investigated the reaction of $Fe_2(CO)_9$ with $Pt(PBu^t_3)_2$ and have obtained $PtFe_2(CO)_9(PBu^t_3)$, **14**, the diiron analogue of **11**. The synthetic and structural details for compounds **10**−**14** and a Fenske−Hall molecular orbital analysis of the bonding interactions of the $Pd(PBu^t_3)$ groups with the Ru−Ru metal−metal bond in **10** are included in this paper.

Experimental Section

General Information. All reactions were performed under a nitrogen atmosphere. Reagent grade solvents were dried by the standard procedures and were freshly distilled prior to use. Infrared spectra were recorded on an Avatar 360 FTIR spectrophotometer. The ^{1}H NMR and ^{31}P NMR were recorded on a Varian Inova 400 spectrometer operating at 400 and 162 MHz, respectively. The ^{31}P NMR spectra were externally referenced against 85% ortho-H_3PO_4. Elemental analyses were performed by Desert Analytics (Tucson, AZ). $Pd(PBu^t_3)_2$, $Pt(PBu^t_3)_2$, $Ru_3(CO)_{12}$, and $Fe_2(CO)_9$ were obtained from Strem and were used without further purification. Product separations were performed by TLC in air on Analtech 0.25 and 0.5 mm silica gel 60 Å F_{254} glass plates.

Preparation of $Ru_2(CO)_9[Pd(PBu^t_3)]_2$, 10. A 11.1 mg sample of $Ru_3(CO)_{12}$ (0.017 mmol) dissolved in 50 mL of hexane was converted into $Ru(CO)_5$ by irradiation (UV) under a CO atmosphere.[13] A 14.0 mg sample of $Pd(PBu^t_3)_2$ (0.027 mmol) was added to the solution at 0 °C, and the solution was then stirred for 3 h, with slow warming to room temperature. The product was separated on a Florisil column to yield 11.5 mg (40% based on Pd) of $Ru_2(CO)_9[Pd(PBu^t_3)]_2$, **10**. IR ($\nu_{CO}$, cm^{-1}, in hexane): 2020 (s), 1997 (vs), 1957 (m), 1931 (m, br), 1870 (w, br). ^{1}H NMR (in $CDCl_3$): δ = 1.48 ppm (d, 54H, CH_3, $^3J_{P-H}$ = 12 Hz). ^{31}P{^{1}H} NMR (in

(12) (a) Adams, R. D.; Captain, B.; Fu, W.; Smith, M. D. *J. Am. Chem. Soc.* **2002**, *124*, 5628. (b) Adams, R. D.; Captain, B.; Fu, W.; Pellechia, P. J.; Smith, M. D. *Angew. Chem., Int. Ed.* **2002**, *41*, 1951. (c) Adams, R. D.; Captain, B.; Fu, W.; Pellechia, P. J.; Smith, M. D. *Inorg. Chem.* **2003**, *42*, 2094. (d) Adams, R. D.; Captain, B.; Fu, W.; Smith, M. D. *J. Organomet. Chem.* **2003**, *682*, 113. (e) Adams, R. D.; Captain, B.; Zhu, L. *J. Am. Chem. Soc.* **2004**, *126*, 3042.
(13) Huq, R.; Poe, A. J.; Chawla, S. *Inorg. Chim. Acta* **1980**, *38*, 121.

$CDCl_3$): δ = 81.03 ppm. Anal. Calcd: C, 36.98; H, 5.04. Found: C, 36.71; H, 5.12.

Preparation of $PtRu_2(CO)_9(PBu^t_3)$, 11, and $Ru_2(CO)_9[Pt(PBu^t_3)]_2$, 12. A 11.1 mg sample of $Ru_3(CO)_{12}$ (0.017 mmol) was converted into $Ru(CO)_5$ by irradiation (UV) under a CO atmosphere. A 17.2 mg sample of $Pt(PBu^t_3)_2$ (0.029 mmol) was then added to the solution at 0 °C, and the solution was then stirred for 3 h, with slow warming to room temperature. The product was separated on TLC using a 3:1 hexane/methylene chloride solvent mixture to yield 5.0 mg (20% based on Pt) of $PtRu_2(CO)_9(PBu^t_3)$, **11**, and 12.2 mg (33% based on Pt) of $Ru_2(CO)_9[Pt(PBu^t_3)]_2$, **12**. The following are the spectral data for **11**. IR (ν_{CO}, cm^{-1}, in hexane): 2090 (m), 2070 (w), 2040 (vs), 2029 (m), 2023 (m), 2010 (vs), 1995(w), 1975 (m), 1957 (w, br), 1840 (w), 1818 (w). ^1H NMR (in $CDCl_3$): δ = 1.54 ppm (d, 27H, CH_3, $^3J_{P-H}$ = 13 Hz). $^{31}P\{^1H\}$ NMR (in $CDCl_3$): δ = 111.78 ppm ($^1J_{Pt-P}$ = 3514 Hz). Anal. Calcd: C, 29.61; H, 3.17. Found: C, 29.56; H, 3.09. The following are the spectral data for **12**. IR (ν_{CO}, cm^{-1}, in CH_2Cl_2): 2066 (w), 2001 (vs), 1968 (m), 1805 (w, br). ^1H NMR (in $CDCl_3$): δ = 1.52 ppm (d, 54H, CH_3, $^3J_{P-H}$ = 13 Hz). $^{31}P\{^1H\}$ NMR (in $CDCl_3$): δ = 110.33 ppm ($^1J_{Pt-P}$ = 5582 Hz). Anal. Calcd: C, 31.73; H, 4.33. Found: C, 31.54; H, 4.24.

Conversion of 11 to 12. A 15.7 mg sample of **11** (0.018 mmol) dissolved in 15 mL of CH_2Cl_2 was allowed to react with 12.0 mg of $Pt(PBu^t_3)_2$ (0.020 mmol) at room temperature for 30 min. The solution was concentrated, and the product was separated on a TLC plate to yield 13.8 mg of **12** (61%).

Preparation of $Pt_2Ru_2(CO)_8(PBu^t_3)_2(\mu\text{-}H)_2$, 13. A 22.0 mg sample of **12** was dissolved in 40 mL of hexane in a 100 mL three-neck round-bottom flask equipped with a stir bar, reflux condenser, and gas inlet. The solution was then purged with hydrogen (1 atm) for 30 min at 68 °C. After filtration, the solvent was removed and the residues were recrystallized from a hexane/methylene chloride solvent mixture to yield 13.8 mg of $Pt_2Ru_2(CO)_8(PBu^t_3)_2(\mu\text{-}H)_2$, **13** (64% yield). Compound **13** can be purified by chromatography on silica gel if desired. IR (ν_{CO}, cm^{-1}, in CH_2Cl_2): 2053 (m), 2018 (s), 1981 (m,sh) 1947 (m, sh). ^1H NMR (in $CDCl_3$): δ = 1.41 ppm (d, 56H, CH_3, $^3J_{P-H}$ = 12 Hz), δ = −8.76 ppm (d, 2H, μ-H, $^2J_{P-H}$ = 15 Hz, $^1J_{Pt-H}$ = 250 Hz). Anal. Calcd: C, 31.40; H, 4.58. Found: C, 31.60; H, 4.77.

Preparation of $PtFe_2(CO)_9(PBu^t_3)$, 14. A 14.7 mg sample of $Fe_2(CO)_9$ (0.040 mmol) was dissolved in 15 mL of CH_2Cl_2. A 25.0 mg sample of $Pt(PBu^t_3)_2$ (0.042 mmol) was then added, and the reaction mixture was stirred at room temperature for 20 min. Within 1 min the color of the solution turned to bright red. The solvent was removed in vacuo, and the residue was dissolved in CH_2Cl_2 and separated by TLC using a 4:1 hexane/methylene chloride solvent mixture to yield 10.2 mg (33%) of $PtFe_2(CO)_9(PBu^t_3)$, **14**. IR (ν_{CO}, cm^{-1}, in hexane): 2074 (m), 2021 (s), 2009 (m), 1991 (m), 1969 (w), 1918 (vw, br). ^1H NMR (in $CDCl_3$): δ = 1.55 ppm (d, 27H, CH_3, $^3J_{P-H}$ = 13 Hz). $^{31}P\{^1H\}$ NMR (in $CDCl_3$): δ = 121.78 ppm ($^1J_{Pt-P}$ = 3121 Hz). Anal. Calcd: C, 33.11; H, 3.54. Found: C, 33.01; H, 3.31.

Table 1. Crystallographic Data for Compounds **10** and **11**

	10	**11**
empirical formula	$Pd_2Ru_2P_2O_9C_{33}H_{54}$	$PtRu_2PO_9C_{21}H_{27}$
fw	1071.64	851.63
cryst syst	monoclinic	monoclinic
lattice params		
a (Å)	8.6504(10)	16.3910(9)
b (Å)	14.4307(17)	8.4841(4)
c (Å)	32.545(4)	20.8710(11)
α (deg)	90	90
β (deg)	95.003(3)	110.737(1)
γ (deg)	90	90
V (Å^3)	4047.2(8)	2714.4(2)
space group	$P2_1/n$ (No. 14)	$P2_1/n$ (No. 14)
Z	4	4
ρ_{calcd} (g/cm^3)	1.759	2.084
μ(Mo Kα) (mm^{-1})	1.732	6.343
temp (K)	190	296
$2\theta_{max}$ (deg)	52.88	50.04
no. of obsd reflns ($I > 2\sigma(I)$)	5823	4337
no. of params	451	316
GOF[a]	1.002	1.060
max shift in cycle	0.001	0.001
residuals:[a] R1; wR2	0.0439; 0.0815	0.0328; 0.0816
abs correction, max/min	SADABS 0.89/0.53	SADABS 1.000/0.609
largest peak in final difference map (e$^-$/Å^3)	0.968	1.646

[a] $R1 = \sum_{hkl}(||F_o| - |F_c||)/\sum_{hkl}|F_o|$; $wR2 = [\sum_{hkl}w(|F_o| - |F_c|)^2/\sum_{hkl}wF_o^2]^{1/2}$, $w = 1/\sigma^2(F_o)$; $GOF = [\sum_{hkl}w(|F_o| - |F_c|)^2/(n_{data} - n_{vari})]^{1/2}$.

Crystallographic Analysis. Orange-red single crystals of **10**−**14** suitable for diffraction analysis were grown by slow evaporation of solvent from solutions of each pure compound in hexane/methylene chloride solvent mixtures at 5 °C. Each data crystal was glued onto the end of a thin glass fiber. X-ray intensity data were measured at 190 or 293 K by using a Bruker SMART APEX CCD-based diffractometer and Mo Kα radiation (λ = 0.71073 Å). The raw data frames were integrated with the SAINT+ program using a narrow-frame integration algorithm.[14] Correction for the Lorentz and polarization effects was also applied by SAINT. An empirical absorption correction based on the multiple measurement of equivalent reflections was applied by using the program SADABS. Crystal data, data collection parameters, and the results of the analyses are listed in Tables 1 and 2.

Compounds **10**−**12** and **14** crystallized in the monoclinic crystal system. The space group $P2_1/n$ was established by the systematic absences in the data and confirmed by the successful solution and refinement of the structure. All the non-hydrogen atoms were refined with anisotropic thermal parameters. The structures were solved by a combination of direct methods and difference Fourier syntheses, and refined by the full-matrix least-squares method on F^2, by using the SHELXTL software package.[15] Hydrogen atoms were placed in geometrically idealized positions and refined as standard riding atoms.

Compound **13** crystallized in the triclinic crystal system. The space group $P\bar{1}$ was assumed and confirmed by the successful solution and refinement of the structure. All the

(14) *SAINT+*, version 6.02a; Bruker Analytical X-ray System, Inc.: Madison, WI, 1998.
(15) Sheldrick, G. M. *SHELXTL*, version 5.1; Bruker Analytical X-ray Systems, Inc.: Madison, WI, 1997.

Table 2. Crystallographic Data for Compounds **12**−**14**

	12	**13**	**14**
empirical formula	$Pt_2Ru_2P_2O_9C_{33}H_{54}$	$Pt_2Ru_2P_2O_8C_{32}H_{56}$	$PtFe_2PO_9C_{21}H_{27}$
fw	1249.02	1223.03	761.19
cryst syst	monoclinic	triclinic	monoclinic
lattice params			
a (Å)	14.5394 (10)	10.8083 (7)	16.2566(8)
b (Å)	16.2556 (11)	13.6810 (9)	8.3777(4)
c (Å)	17.0963 (12)	14.7861(10)	20.4807(10)
α (deg)	90	96.124(2)	90
β (deg)	90.262(1)	95.480(2)	110.7010(10)
γ (deg)	90	108.631(2)	90
V (Å^3)	4040.6(5)	2040.4(2)	2609(2)
space group	$P2_1/n$ (No. 14)	$P\bar{1}$ (No. 2)	$P2_1/n$ (No. 14)
Z	4	2	4
ρ_{calcd} (g/cm^3)	2.053	1.991	1.938
μ(Mo Kα) (mm^{-1})	7.762	7.681	6.552
temp (K)	190	296	296
$2\theta_{max}$ (deg)	50.06	50.06	52.04
no. of obsd reflns ($I > 2\sigma(I)$)	6140	5898	4678
no. of params	451	441	316
GOF[a]	0.984	1.019	1.035
max shift in cycle	0.004	0.001	0.006
residuals:[a] R1; wR2	0.0254; 0.0563	0.0399; 0.0892	0.0184; 0.0439
abs correction, max/min	SADABS 0.414/0.292	SADABS 1.000/0.667	SADABS 1.000/0.681
largest peak in final difference map (e$^-$/Å^3)	1.021	2.242	0.517

[a] $R1 = \sum_{hkl}(||F_o| - |F_c||)/\sum_{hkl}|F_o|$; $wR2 = [\sum_{hkl}w(|F_o| - |F_c|)^2/\sum_{hkl}wF_o^2]^{1/2}$, $w = 1/\sigma^2(F_o)$; $GOF = [\sum_{hkl}w(|F_o| - |F_c|)^2/(n_{data} - n_{vari})]^{1/2}$.

non-hydrogen atoms were refined with anisotropic thermal parameters. The structure was solved by a combination of direct methods and difference Fourier syntheses, and refined by the full-matrix least-squares method on F^2, by using the SHELXTL software package.[15] The hydride ligands were located and refined with isotropic thermal parameters. Hydrogen atoms were placed in geometrically idealized positions and refined as standard riding atoms.

Molecular Orbital Calculations. All molecular orbital calculations reported here were performed by using the Fenske−Hall method.[16] Fenske−Hall calculations were performed by utilizing a graphical user interface developed[17] to build inputs and view outputs from stand-alone Fenske−Hall (version 5.2) and MOPLOT2[18] binary executables. Contracted double-ζ basis sets were used for the Ru and Pd 4d, P 3p, and C and O 2p atomic orbitals. The Fenske−Hall scheme is a nonempirical, approximate method that is capable of calculating molecular orbitals for very large transition-metal systems and has built-in fragment analysis routines that allow one to assemble transition-metal cluster structures from the corresponding ligated fragments.

Results and Discussion

The reaction of $Ru(CO)_5$ with $Pd(PBu^t_3)_2$ at room temperature afforded the dipalladium−diruthenium complex $Ru_2(CO)_9[Pd(PBu^t_3)]_2$, **10**, in 40% yield; see eq 1. Compound

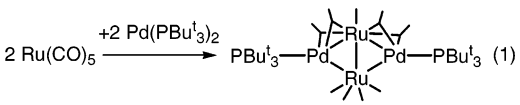

10

10 was characterized by a combination of IR, ^{1}H and ^{31}P NMR, and single-crystal X-ray diffraction analyses. An ORTEP diagram of the molecular structure of **10** is shown in Figure 1. Selected intramolecular distances and angles are listed in Table 3.

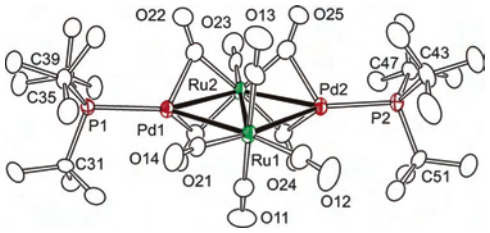

Figure 1. An ORTEP diagram of $Ru_2(CO)_9[Pd(PBu^t_3)]_2$, **10**, showing 40% probability thermal ellipsoids.

This compound contains two ruthenium atoms joined by a Ru−Ru single bond, Ru−Ru = 3.0114(7) Å. There are also two $Pd(PBu^t_3)$ groups that bridge the two ruthenium atoms on opposite sides of the molecule. The ruthenium atom Ru(2) has five carbonyl ligands, four of which bridge to the neighboring Pd atoms. Ru(1) on the other hand has only four carbonyl ligands, all of which are terminally coordinated. The Ru(2)−Pd bond distances of 2.7863(7) and 2.7694(6) Å are shorter than the Ru(1)−Pd bond distances, 2.8009(6) and 2.8207(7) Å. The shortness of the Ru(2)−Pd bonds can be attributed to the presence of the bridging carbonyl ligands on those bonds. With nine CO ligands, compound **10** can be viewed as a dipalladium adduct of the compound $Ru_2(CO)_9$. $Ru_2(CO)_9$ was first obtained by the photodecarbonylation of $Ru(CO)_5$ in 1977 and was reported to be "very unstable" at room temperature.[19] A determination of the

(16) Hall, M. B.; Fenske, R. F. *Inorg. Chem.* **1972**, *11*, 768.
(17) Manson, J.; Webster, C. E.; Hall, M. B. *JIMP*, development version 0.1 (built for Windows PC and Redhat Linux 7.3); Department of Chemistry, Texas A&M University: College Station, TX, March 2003 (http://www.chem.tamu.edu/jimp/).
(18) Lichtenberger, D. L. *MOPLOT2: for orbital and density plots from linear combinations of Slater or Gaussian type orbitals*, version 2.0; Department of Chemistry, University of Arizona: Tucson, AZ, June 1993.

Scheme 1

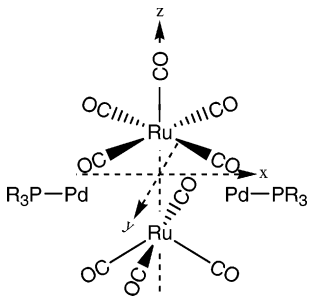

molecular structure of $Ru_2(CO)_9$ by X-ray crystallographic methods has not yet been reported.

Simple Lewis acid−base bonding models were proposed to describe the bonding interactions of the $Pd(PBu^t_3)$ groups with the $Ru_2(CO)_9$ unit.[12a] The nature of the bonding interactions has now been investigated in more detail by molecular orbital calculations and is as follows. One can envision the $Ru_2(CO)_9[Pd(PR_3)]_2$ cluster (Scheme 1) being assembled from two ruthenium fragments, $Ru(CO)_4$ and $Ru(CO)_5$, and two $Pd(PR_3)$ fragments; the orbital representations in Scheme 2 are idealized. The coordinate system chosen for the $Ru_2(CO)_9[Pd(PR_3)]_2$ cluster corresponds to its approximate C_2 point group, and this choice has been carried over to the coordinate systems of the fragments (Scheme 1). While this coordinate choice does not have the ligands aligned with the Cartesian axes and changes the usual representation of the t_{2g} (d_{xy}, d_{xz}, and d_{yz}) and e_g (d_{z^2} and $d_{x^2-y^2}$) sets of orbitals for an octahedral metal, the bonding description remains unaffected, aside from labeling. The key low-lying orbitals for $Pd(PR_3)$, $Ru(CO)_5$, and $Ru(CO)_4$ units are illustrated in Scheme 2 (in the orientation of the $Ru_2(CO)_9$-$[Pd(PR_3)]_2$ complex shown in Scheme 1). The key orbitals of the d^{10} $Pd(PR_3)$ fragment are the LUMO, the "sp" hybrid, and the five occupied d orbitals, especially the HOMO, the "d_{z^2}" orbital (see Scheme 2). In the neutral, d^8 $Ru(CO)_5$ fragment (Scheme 2), the d orbitals form two sets reflecting the character of their octahedral parentage: (1) three low-lying occupied orbitals ($d_{x^2-y^2}$, d_{xz}, and d_{yz}) are stabilized by the carbonyl π^* orbital as in the parent octahedral t_{2g} set and (2) one occupied orbital, the HOMO (d_{z^2}), and one very high lying unoccupied orbital (d_{xy}, not pictured in Scheme 2) are each destabilized by the carbonyl σ orbital as in the parent octahedral e_g set. Removing one CO from the $Ru(CO)_5$ fragment generates the d^8 $Ru(CO)_4$ fragment (Scheme 2) whose five orbitals with t_{2g} and e_g parentage are three low-lying orbitals (d_{xy}, d_{yz}, and d_{z^2}), the HOMO (d_{xz}), and one high-lying unoccupied orbital ($d_{x^2-y^2}$, not pictured in Scheme 2). There is considerable p character in the HOMO of

Table 3. Selected Intramolecular Bond Distances and Angles for Compound **10**[a]

atom	atom	distance (Å)	atom	atom	distance (Å)
Pd(1)	Ru(1)	2.8009(6)	Ru(2)	C(22)	2.043(6)
Pd(1)	Ru(2)	2.7863(7)	Pd(1)	C(21)	2.287(7)
Pd(2)	Ru(1)	2.8207(7)	Ru(2)	C(21)	1.998(6)
Pd(2)	Ru(2)	2.7694(6)	Pd(2)	C(24)	2.164(6)
Ru(1)	Ru(2)	3.0114(7)	Ru(2)	C(24)	2.010(6)
Pd(1)	P(1)	2.3971(13)	Pd(2)	C(25)	2.085(6)
Pd(2)	P(2)	2.3873(13)	Ru(2)	C(25)	2.035(6)
Pd(1)	C(22)	2.050(6)	O	C(av)	1.140(7)

atom	atom	atom	angle (deg)	atom	atom	atom	angle (deg)
Pd(1)	Ru(1)	Pd(2)	113.5 1(2)	Ru(2)	Pd(2)	Ru(1)	65.181(17)
Pd(2)	Ru(2)	Pd(1)	115.6 2(2)	P(1)	Pd(1)	Ru(2)	144.19(4)
Ru(2)	Pd(1)	Ru(1)	65.22 7(17)	P(2)	Pd(2)	Ru(1)	148.14(4)

[a] Estimated standard deviations in the least significant figure are given in parentheses.

Scheme 2

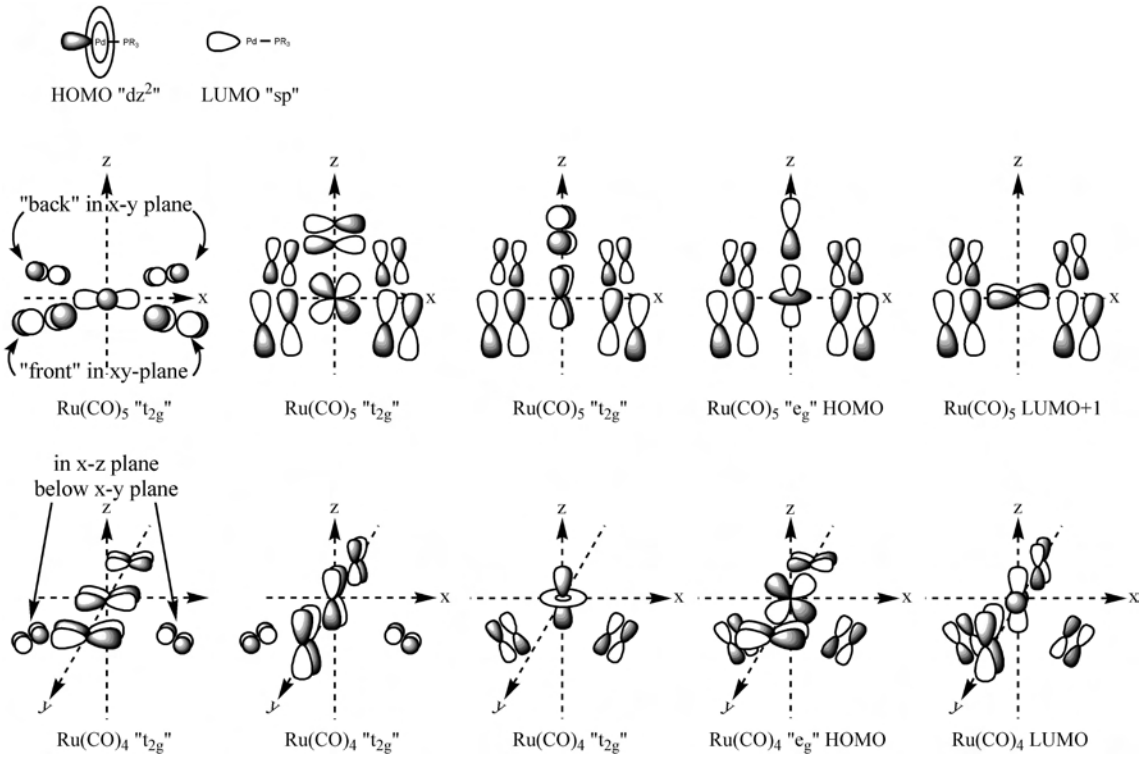

Scheme 3

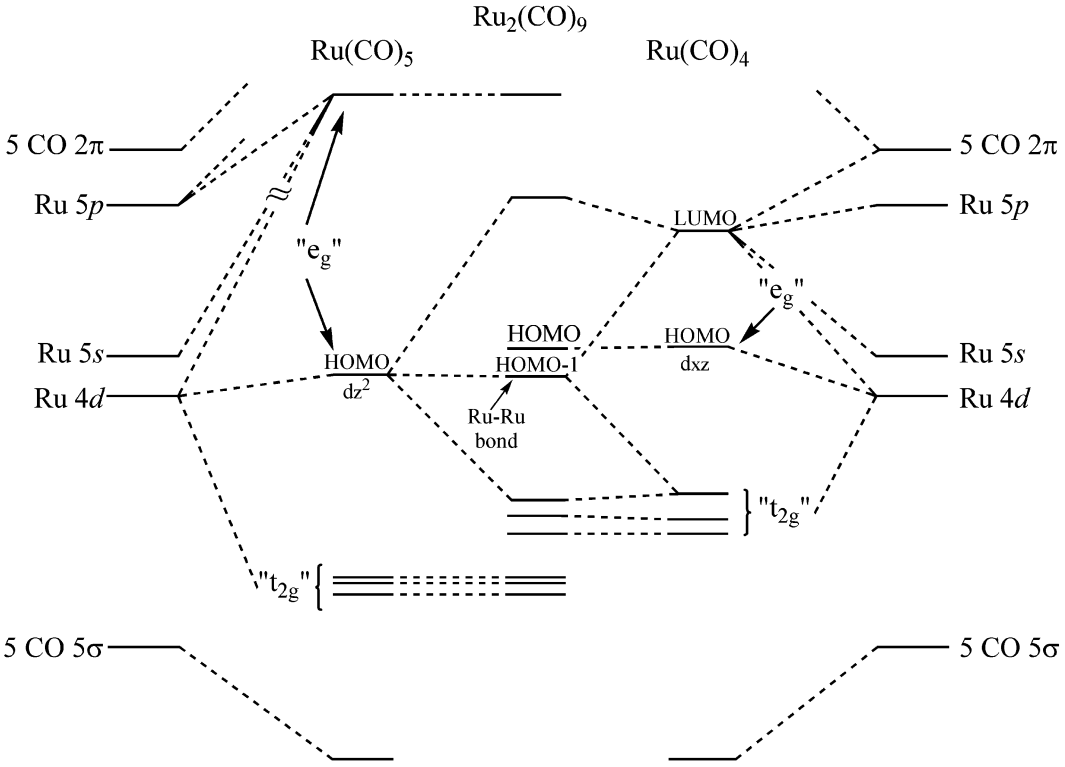

$Ru(CO)_5$ and $Ru(CO)_4$, the LUMO + 1 of $Ru(CO)_5$, and the LUMO of $Ru(CO)_4$. The idealized orbitals shown in Scheme 2 do not reflect all these orbital contributions. For example, the LUMO of the $Ru(CO)_4$ fragment has an important contribution from an sp^2 hybrid pointing in the *z* direction in addition to the $d_{x^2-y^2}$ and d_{z^2} contribution shown in Scheme 2.

The MO diagram for the construction of the two Ru fragments $Ru(CO)_5$ and $Ru(CO)_4$ is given in Scheme 3 on the left and right, respectively. Combining these two ruthenium fragments produces a Ru−Ru metal−metal bond in the $Ru_2(CO)_9$ unit, arising primarily from donation of the electron pair in the HOMO of $Ru(CO)_5$ to the LUMO of $Ru(CO)_4$ (see Scheme 3). The $Ru_2(CO)_9$ unit can then be combined with the two $PdPR_3$ fragments (see Scheme 4). The formation of the $[Pd(PR_3)]_2$ unit is shown on the right of Scheme 4. The four low-lying occupied orbitals form a closely spaced band of eight orbitals. The $Pd(PR_3)$ fragment's d_{z^2} orbitals form the HOMO and HOMO − 1, while the LUMOs of the individual $PdPR_3$ fragments form the LUMO and LUMO + 1 of this Pd_2 unit. The principal bonding interactions between the $Ru_2(CO)_9$ and $[Pd(PR_3)]_2$ units form when the HOMO and HOMO − 1 of the $Ru_2(CO)_9$ unit donate to the LUMO and LUMO + 1 of the $[Pd(PR_3)]_2$ unit, respectively. In this process, the two resulting orbitals localize closer to each Ru center to produce two three-center, two-electron bonds (see Figure 2): the cluster's HOMO primarily bonds the $Ru(CO)_4$ fragment with the antisymmetric combination from the frontier of the two Pd fragments, and the cluster's HOMO − 1 primarily bonds the $Ru(CO)_5$ fragment

Scheme 4

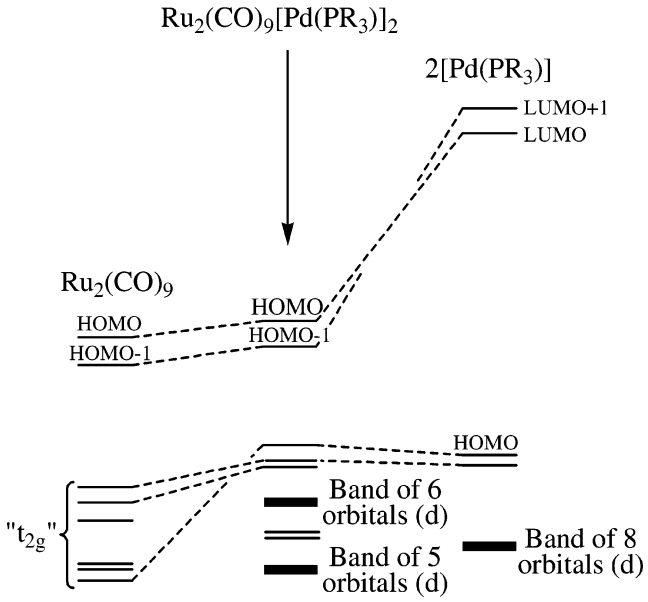

with the symmetric combination from the unoccupied frontier of the two Pd fragments (there is a small contribution from the Ru of the $Ru(CO)_4$ fragment, which gives this bond a small amount of four-center character). For the most part, the lower occupied d orbitals are uninvolved, except for one of the occupied pairs from the $[PdPR_3]_2$ unit that mixes with the $Ru(CO)_4$ fragment's HOMO. This mixing appears in the cluster's HOMO (Figure 2) as small out-of-phase contributions at each Pd.

The $Ru_2(CO)_9$ unit also presents π^* orbitals from six semibridging carbonyls (four from the top $Ru(CO)_5$ fragment and two from the bottom $Ru(CO)_4$ fragment) to the occupied

(19) Moss, J. R.; Graham, W. A. G. *J. Chem. Soc., Dalton Trans.* **1977**, 95.

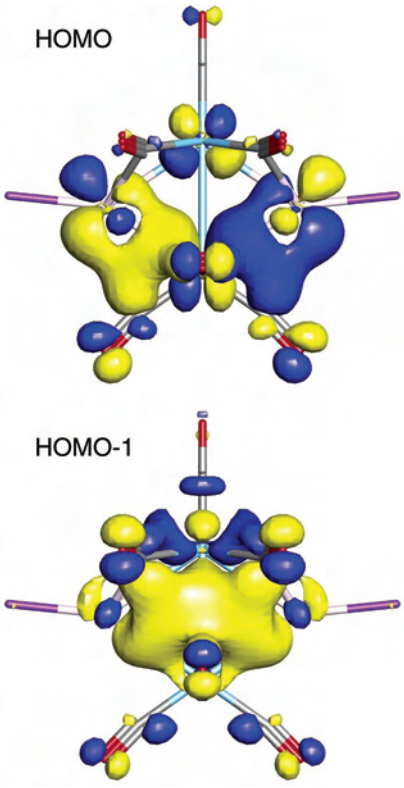

Figure 2. HOMO and HOMO − 1 of the $Ru_2(CO)_9[Pd(PR_3)]_2$ cluster. These orbitals are three-center two-electron bonds, the HOMO is the $Ru(CO)_4$ fragment interacting with the antisymmetric combination of the two Pd fragment LUMO orbitals, and the HOMO − 1 is the $Ru(CO)_5$ fragment interacting with the symmetric combination of the two Pd fragment LUMO orbitals.

Scheme 5

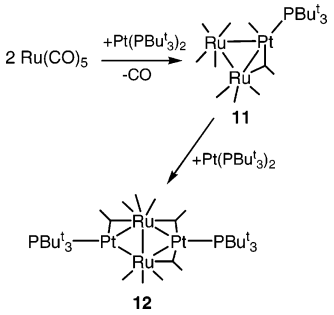

$Pd(PR_3)$ fragment d orbitals. Donation from the occupied Pd d orbitals contributes to the stability of the complex. The LUMO + 1 of $Ru(CO)_5$ and the LUMO of $Ru(CO)_4$ (pictured diagrammatically in Scheme 2) are representatives of these π^* carbonyl orbitals.

$Pt(PBu^t_3)_2$ reacts with $Ru(CO)_5$ to yield the diplatinum−diruthenium complex $Ru_2(CO)_9[Pt(PBu^t_3)]_2$, **12**, in 33% yield, but in addition has also yielded the monoplatinum−diruthenium complex $PtRu_2(CO)_9(PBu^t_3)$, **11**, in 20% yield (see Scheme 5). Both compounds were characterized by a combination of IR, ^1H and ^{31}P NMR, and single-crystal X-ray diffraction analyses. An ORTEP diagram of the molecular structure of **11** is shown in Figure 3. Selected bond distances and angles are listed in Table 4. Compound **11** contains a triangle of three metal atoms, two ruthenium and one platinum, with a carbonyl group bridging the Ru(1)−Pt(1) bond. However, the bridging CO ligand can be considered more as semibridging, Ru(1)−C(14) −O(14) = 168.6(5)°, Pt−C(14)−O(14) = 114.4(4)°. The platinum atom not only is coordinated by the PBu^t_3 group, but also has one terminal carbonyl ligand. The Ru(1)−Ru(2) bond distance of 2.8340(6) Å is shorter than the Ru(1)−Ru(2) distance in **10** due to less donation of electrons from the Ru(1)−Ru(2) bond to the platinum atom. Both ruthenium atoms are coordinated by four CO ligands, and these CO ligands prefer terminal coordination. Compound **11** could be viewed as a combination of $Ru_2(CO)_9$ and $Pt(PBu^t_3)$ groupings, but in this case one of the CO ligands has been transferred completely to the $Pt(PBu^t_3)$ group.

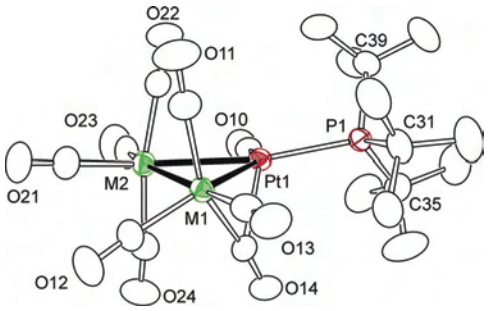

Figure 3. An ORTEP diagram of $PtM_2(CO)_9(PBu^t_3)$, **11** and **14,** M = Ru and Fe, showing 40% probability thermal ellipsoids.

Table 4. Selected Intramolecular Bond Distances and Angles for Compounds **11** and **14**[a]

compound **11**			compound **14**		
atom	atom	distance (Å)	atom	atom	distance (Å)
Pt(1)	Ru(1)	2.7396(5)	Pt(1)	Fe(1)	2.6084(4)
Pt(1)	Ru(2)	2.7408(5)	Pt(1)	Fe(2)	2.6432(4)
Ru(1)	Ru(2)	2.8340(6)	Fe(1)	Fe(2)	2.7188(6)
Pt(1)	P(1)	2.3949(14)	Pt(1)	P(1)	2.4021(7)
Pt(1)	C(14)	2.428(6)	Pt(1)	C(14)	2.343(3)
Ru(1)	C(14)	1.928(6)	Fe(1)	C(14)	1.804(6)
Pt(1)	C(10)	1.866(6)	Pt(1)	C(10)	1.865(3)
O	C(av)	1.136(7)	O	C(av)	1.135(4)

compound **11**				compound **14**			
atom	atom	atom	angle (deg)	atom	atom	atom	angle (deg)
Ru(1)	Pt(1)	Ru(2)	62.278(14)	Fe(1)	Pt(1)	Fe(2)	62.353(13)
Pt(1)	Ru(1)	Ru(2)	58.882(14)	Pt(1)	Fe(1)	Fe(2)	59.451(12)
Pt(1)	Ru(2)	Ru(1)	58.840(13)	Pt(1)	Fe(2)	Fe(1)	58.196(11)
P(1)	Pt(1)	Ru(1)	116.61(3)	P(1)	Pt(1)	Fe(1)	116.743(19)
Pt(1)	C(14)	Ru(1)	77.0(2)	Pt(1)	C(14)	Fe(1)	76.73(11)

[a] Estimated standard deviations in the least significant figure are given in parentheses.

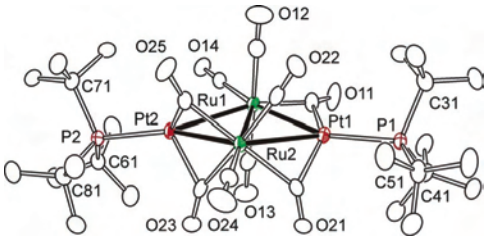

Figure 4. An ORTEP diagram of $Ru_2(CO)_9[Pt(PBu^t_3)]_2$, **12**, showing 40% probability thermal ellipsoids.

Compound **12** was characterized crystallographically, and an ORTEP diagram of its molecular structure is shown in Figure 4. Selected intramolecular distances and angles are

Table 5. Selected Intramolecular Bond Distances and Angles for Compound **12**[a]

atom	atom	distance (Å)	atom	atom	distance (Å)
Pt(1)	Ru(1)	2.6890(4)	Ru(1)	C(11)	1.971(5)
Pt(1)	Ru(2)	2.8584(5)	Pt(1)	C(21)	1.965(5)
Pt(2)	Ru(1)	2.8218(5)	Ru(2)	C(21)	2.162(5)
Pt(2)	Ru(2)	2.7899(4)	Pt(2)	C(23)	2.104(5)
Ru(1)	Ru(1)	2.9724(6)	Ru(2)	C(23)	2.047(5)
Pt(1)	P(1)	2.3195(13)	Pt(2)	C(25)	2.037(5)
Pt(2)	P(2)	2.3147(1 3)	Ru(2)	C(25)	2.040(5)
Pt(1)	C(11)	2.295(6)	C	O(av)	1.148(6)

atom	atom	atom	angle (deg)	atom	atom	atom	angle (deg)
Pt(1)	Ru(1)	Pt(2)	116.015(15)	Ru(2)	Pt(2)	Ru(1)	63.964(13)
Pt(2)	Ru(2)	Pt(1)	111.694(15)	P(1)	Pt(1)	Ru(2)	138.32(3)
Ru(1)	Pt(1)	Ru(2)	64.715(13)	P(2)	Pt(2)	Ru(2)	149.12(3)

[a] Estimated standard deviations in the least significant figure are given in parentheses.

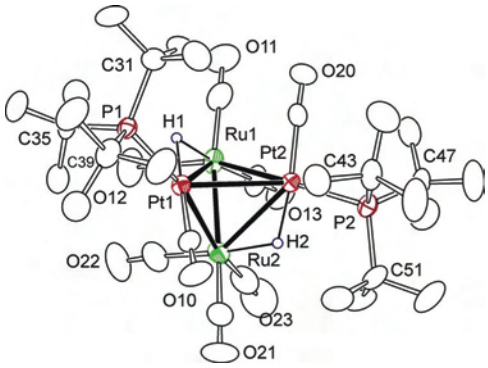

Figure 5. An ORTEP diagram of $Pt_2Ru_2(CO)_8(PBu^t_3)_2(\mu\text{-}H)_2$, **13**, showing 40% probability thermal ellipsoids.

listed in Table 5. The arrangement of the metal atoms in **12** is similar to that in **10**. The Ru−Ru bond length, 2.9724(6) Å, is similar to that of **10**, but is longer than that of **11**. As in compound **10**, one ruthenium atom, Ru(2), contains five carbonyl ligands, whereas the other, Ru(1), has four; however, in **12**, only three of the CO ligands on Ru(2) bridge to the neighboring Pt atoms and one of the CO ligands on the $Ru(CO)_4$ group has formed a bridge to a neighboring platinum atom, Pt(1). This compound can be viewed as a diplatinum adduct of $Ru_2(CO)_9$. Compound **12** has the same number of cluster valence electrons as **10**. We expect that the metal−metal bonding in **12** is similar to that in **10**, but no calculations were performed on **12** to verify this.

Compound **12** reacts with hydrogen at 1 atm in hexane at 68 °C to afford the tetranuclear metal complex $Pt_2Ru_2(CO)_8(PBu^t_3)_2(\mu\text{-}H)_2$, **13**, in 64% yield. Compound **13** was

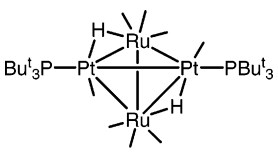

13

characterized by IR, NMR, and single-crystal X-ray diffraction analyses. An ORTEP diagram of the molecular structure of **13** is shown in Figure 5. Selected intramolecular distances and angles are listed in Table 6.

The molecule contains two ruthenium atoms and two platinum atoms in a pseudotetrahedral arrangement. There

Table 6. Selected Intramolecular Bond Distances and Angles for Compound **13**[a]

atom	atom	distance (Å)	atom	atom	distance (Å)
Pt(1)	Pt(2)	3.1462(5)	Pt(2)	P(2)	2.374(2)
Pt(1)	Ru(1)	2.8595(7)	Pt(1)	H(1)	1.73(11)
Pt(1)	Ru(2)	2.7228(8)	Ru(1)	H(1)	1.91(11)
Pt(2)	Ru(1)	2.7217(7)	Pt(2)	H(2)	1.70(8)
Pt(2)	Ru(2)	2.8510(8)	Ru(2)	H(2)	1.83(8)
Ru(1)	Ru(2)	2.7331(11)	O	C(av)	1.134(11)
Pt(1)	P(1)	2.375(2)			

atom	atom	atom	angle (deg)	atom	atom	atom	angle (deg)
Ru(2)	Pt(1)	Ru(1)	58.57(2)	Pt(2)	Ru(1)	Ru(2)	63.02(2)
Ru(2)	Pt(1)	Pt(2)	57.585(17)	Pt(2)	Ru(1)	Pt(1)	68.574(18)
Ru(1)	Pt(1)	Pt(2)	53.639(16)	Ru(2)	Ru(1)	Pt(1)	58.22(2)
Ru(1)	Pt(2)	Ru(2)	58.68(2)	Pt(1)	Ru(2)	Ru(1)	63.22(2)
Ru(1)	Pt(2)	Pt(1)	57.787(17)	Pt(1)	Ru(2)	Pt(2)	68.684(18)
Ru(2)	Pt(2)	Pt(1)	53.730(16)	Ru(1)	Ru(2)	Pt(2)	58.29(2)

[a] Estimated standard deviations in the least significant figure are given in parentheses.

are two hydride ligands (located and refined crystallographically) that bridge two of the Ru−Pt bonds. The hydride-bridged Ru−Pt bond lengths, Ru(1)−Pt(1) = 2.8595(7) Å and Ru(2)−Pt(2) = 2.8510(8) Å, are significantly longer than the unbridged Ru−Pt bond lengths, Ru(1)−Pt(2) = 2.7217(7) Å and Ru(2)−Pt(1) = 2.7228(8) Å, as expected due to bond lengthening effects of bridging hydride ligands.[20] The hydride ligands are equivalent and exhibit only one resonance in the ^{1}H NMR spectrum, $\delta = -8.76$ ppm (d, 2H, μ-H, $^2J_{P-H} =$ 15 Hz, $^1J_{Pt-H} = 250$ Hz). Compound **13** has eight carbonyl ligands: three terminal CO ligands on each ruthenium atom and one on each of the platinum atoms. Compound **13** is similar to the compound $Pt_2Ru_2(CO)_8(PPh_3)_2(\mu\text{-}H)_2$,[21] and the metal−metal bond distances are also similar to those found in $Pt_2Ru_2(CO)_8(PPh_3)_2(\mu\text{-}H)_2$.[21] The valence electron count for **13** is 58, which is 2 less than the expected 60-electron count for closed tetrahedral clusters; however, it has been found that tetrahedral clusters that contain platinum often contain 58 electrons.[22]

Compounds **10**−**12** each contain a diruthenium group obtained from the monoruthenium precursor $Ru(CO)_5$. The diruthenium groups were presumably formed by the combination of 1 equiv of $Ru(CO)_5$ with a $Ru(CO)_4$ fragment formed by loss of CO from a second equivalent of $Ru(CO)_5$. The diruthenium group is then stabilized by the addition of the bridging $M(PBu^t_3)$ groups. In the case of **11** one of the CO groups was shifted to the platinum atom.

Due to the "very unstable" nature of $Ru_2(CO)_9$, it was not possible to perform reactions of $Pd(PBu^t_3)_2$ and $Pt(PBu^t_3)_2$ with $Ru_2(CO)_9$. However, its iron analogue, $Fe_2(CO)_9$, is very stable and readily available. The reaction of $Fe_2(CO)_9$ with $Pt(PBu^t_3)_2$ at room temperature afforded the new complex $PtFe_2(CO)_9(PBu^t_3)$, **14**, in 33% yield. The structure of compound **14** is analogous to that of **11**, and both compounds are isomorphous and isostructural in the solid state (see Figure 3). Selected bond distances and angles for **14** are listed in Table 4. Needless to say, the Fe−Fe and Pt−Fe distances

(20) Teller, R. G.; Bau, R. *Struct. Bonding* **1981**, *41*, 1.
(21) Adams, R. D.; Bunz, U.; Captain, B.; Fu, W.; Steffen, W. *J. Organomet. Chem.* **2000**, 6*14*, 75.
(22) Farrugia, L. J. *Adv. Organomet. Chem.* **1990**, *31*, 301.

in **14** are significantly shorter than those in **11**, because of the smaller size of iron compared to ruthenium. Interestingly, we were not able to obtain compound **14** from a reaction of $Pt(PBu^t_3)_2$ with $Fe(CO)_5$ under conditions similar to those of the $Ru(CO)_5$ reactions. This could be due to the lower reactivity of $Fe(CO)_5$ compared to $Ru(CO)_5$. Also, we were not able to prepare the iron homologue of **12** by reaction of **14** with additional quantities of $Pt(PBu^t_3)_2$. It must be that this compound is simply too unstable. We also found no evidence for the monopalladium homologue of **11** and **14**, $PdRu_2(CO)_9(PBu^t_3)$, under our conditions.

In this work, we have again shown the extraordinary ability of $Pd(PBu^t_3)_2$ and $Pt(PBu^t_3)_2$ to generate $Pd(PBu^t_3)$ and $Pt(PBu^t_3)$ groups by loss of one of their PBu^t_3 ligands. The $Pd(PBu^t_3)$ and $Pt(PBu^t_3)$ groups are readily added across metal−metal bonds to yield stable new bimetallic cluster complexes. In the cases of the ruthenium reactions, the mononuclear metal reagent $Ru(CO)_5$ was readily converted to diruthenium compounds to yield more stable products. Two of these new compounds, **10** and **12**, possess extensive delocalized metal−metal bonding. These reactions should be useful in the preparation of still more types of bimetallic clusters with delocalized metal−metal bonding that may also be good precursors to bimetallic nanoparticles and supported bimetallic catalysts.[9]

Acknowledgment. This research was supported by the Office of Basic Energy Sciences of the U.S. Department of Energy under Grant No. DE-FG02-00ER14980. We thank Strem for donation of a sample of $Pt(PBu^t_3)_2$. The work at Texas A&M University (TAMU) was supported by the NSF (Grant CHE98-00184), The Welch Foundation (Grant A-0648), and TAMU.

Supporting Information Available: CIF files for each of the structural analyses. This material is available free of charge via the Internet at http://pubs.acs.org.

IC049675J